Biochimica et Biophysica Acta 1863 (2016) 1624–1632

Contents lists available at ScienceDirect

Biochimica et Biophysica Acta

journal homepage: www.elsevier.com/locate/bbamcr

Cox26 is a novel stoichiometric subunit of the yeast cytochrome *c* oxidase

Maria Levchenko [a], Jan-Moritz Wuttke [a], Katharina Römpler [a], Bernhard Schmidt [a], Klaus Neifer [a], Lisa Juris [a], Mirjam Wissel [a], Peter Rehling [a,b,*], Markus Deckers [a]

[a] Department of Cellular Biochemistry, University Medical Center Göttingen, D-37073 Göttingen, Germany
[b] Max Planck Institute for Biophysical Chemistry, D-37077 Göttingen, Germany

ARTICLE INFO

Article history:
Received 8 January 2016
Received in revised form 31 March 2016
Accepted 6 April 2016
Available online 12 April 2016

ABSTRACT

The cytochrome *c* oxidase (COX) is the terminal enzyme of the respiratory chain. The complex accepts electrons from cytochrome *c* and passes them onto molecular oxygen. This process contributes to energy capture in the form of a membrane potential across the inner membrane. The enzyme complex assembles in a stepwise process from the three mitochondria-encoded core subunits Cox1, Cox2 and Cox3, which associate with nuclear-encoded subunits and cofactors. In the yeast *Saccharomyces cerevisiae*, the cytochrome *c* oxidase associates with the bc_1-complex into supercomplexes, allowing efficient energy transduction. Here we report on Cox26 as a protein found in respiratory chain supercomplexes containing cytochrome *c* oxidase. Our analyses reveal Cox26 as a novel stoichiometric structural subunit of the cytochrome *c* oxidase. A loss of Cox26 affects cytochrome *c* oxidase activity and respirasome organization.

1. Introduction

Cellular processes require energy to drive chemical, osmotic, and mechanical work. Mitochondria contribute to cellular energy homeostasis by production of ATP via oxidative phosphorylation. This process depends on the respiratory chain in the mitochondrial inner membrane that transfers electrons from reducing equivalents to molecular oxygen. The energy of this electron flux is used to generate the membrane potential across the mitochondrial inner membrane that drives ATP synthesis by the F_1F_o-ATPase. The oxidative phosphorylation system (OXPHOS) in *Saccharomyces cerevisiae* consists of single NADH dehydrogenases and four multi subunit complexes (complexes II–V) [1–5]. These complexes, with the exception of complex II, are composed of subunits encoded by both the mitochondrial and nuclear genomes [6]. Studies on the assembly of complexes III and IV showed a stepwise association of single components to a core structure of proteins formed by mitochondrial translation products [7–10]. Mitochondrial translation takes place at the inner mitochondrial membrane and is regulated by subunit-specific translation activators that interact with the respective mRNA molecules [11]. The nascent polypeptides are inserted into the membrane in a co-translational manner with the help of the Oxa1 (oxidase assembling 1 translocase) insertase [12,13]. Nuclear-encoded assembly factors associate with these translation products and promote further maturation of the respiratory chain complexes. During the assembly process, cofactors need to be incorporated stepwise into the "growing" enzymes [14]. The assembly factors play a critical role in these processes defining an assembly line. Similar to the majority of structural subunits, the assembly factors are translated on cytosolic ribosomes and transported into mitochondria.

The assembly of respiratory chain complexes is a process that extends beyond the formation of the mature and functional individual enzymes. In fact, respiratory chain complexes have been found to form higher oligomers in the inner membrane termed respirasomes or supercomplexes [15–18]. In the case of the yeast *S. cerevisiae*, respiratory chain complexes III and IV form a higher oligomeric structure consisting of two copies of complex III with one or two copies of complex IV. Respiratory chain supercomplex formation allows efficient energy transduction between the bc_1-complex (complex III) and the cytochrome *c* oxidase (complex IV) [19–23]. While cardiolipin has been found to stabilize respiratory chain complexes, recent studies have identified Rcf1 as a supercomplex oligomerization factor [24–28].

In a proteomic characterization of purified respiratory chain supercomplexes we identified an uncharacterized protein YDR119W-A (Cox26) [26]. Our study verified the supercomplex association of Cox26. We find that Cox26 is a stoichiometric complex IV subunit. Cox26-containing complex IV is incorporated into respirasomes by an association with the dimer of complex III. This supercomplex formation is altered in the absence of Cox26 and leads to increased monomeric complex IV and a slight decrease in cytochrome *c* oxidase enzyme activity. Our analysis demonstrates that besides the known structural subunits of complex IV Cox26 is a novel constituent. We conclude that in addition

* Corresponding author at: Department of Cellular Biochemistry, University Medical Center Göttingen, D-37073 Göttingen, Germany. Tel.: +49 551 395948; fax: +49 551 395979.
E-mail address: peter.rehling@medizin.uni-goettingen.de (P. Rehling).

http://dx.doi.org/10.1016/j.bbamcr.2016.04.007
0167-4889/

to the described complex IV subunits so far unidentified, stoichiometric and sub-stoichiometric subunits may exist that are necessary to regulate the enzyme function and proper insertion into respirasomes.

2. Materials and methods

2.1. Yeast strains and growth conditions

Yeast strains used in this study are derivatives of *S. cerevisiae* strain YPH499 [29] and are listed in Table 1. Deletion of *COX26* was achieved by homologous recombination of a *KANMX6* cassette into the corresponding locus. Generation of tagged strains was performed by chromosomal integration [30,31]. Cox4^{ZZ}, *cyt1*Δ, and *cox4*Δ were described previously [26,32]. All yeast strains were grown on rich medium (1% yeast extract, 2% peptone) supplemented with 3% glycerol or 2% glucose, unless stated otherwise. Mitochondria were isolated from yeast grown at 30 °C in rich liquid medium containing 1% yeast extract, 2% peptone and 3% glycerol, or 2% galactose in the case of strains affected in respiratory chain function as previously described [33]. For growth tests, yeast cells from liquid cultures were adjusted to an OD_{600} of 0.3 and serial dilutions of the cultures were spotted onto agar plates containing glucose or glycerol as a carbon source and incubated at indicated temperatures.

2.2. Fluorescence microscopy

For fluorescence microscopy analysis, yeast cells expressing Cox26-^{GFP} were grown in minimal medium supplemented with 2% galactose to mid-log phase at 30 °C. Cells were stained with 500 nM MitoTracker® Orange CMTMRos probe (Invitrogen) for 20 min at 30 °C in the dark and used for fluorescence microscopy. Images were collected by using a DeltaVision microscope (Olympus IX71, Applied Precision, Issaquah, WA, USA) and deconvoluted by using Softworx, version 3.5.1 (Great Falls, MT, USA).

2.3. Protein localization assays

Analyses were performed essentially as previously described [26]. For membrane-association analysis isolated mitochondria containing Cox26^{FLAG} were subjected to extraction in 0.1 M Na_2CO_3 (pH 10.8), or lysed with 0.1% Triton X-100 supplemented with 0.4 M KCl. Membranes and soluble fractions were separated by centrifugation for 1 h at 100,000 rpm, 4 °C in a TLA-55 rotor (Beckmann). Samples were precipitated with trichloroacetic acid (TCA) and analyzed by SDS-PAGE and Western-blotting. For protease protection assays mitochondria were resuspended in iso-osmotic SEM buffer (250 mM sucrose, 1 mM EDTA, 10 mM MOPS, pH 7.2), converted to mitoplasts by hypotonic swelling in EM buffer (1 mM EDTA, 10 mM MOPS, pH 7.2), or lysed in 0.2% Triton X-100 for 20 min on ice and subsequently treated with indicated amounts of proteinase K (PK) for 10 min on ice. Samples were precipitated with TCA and analyzed by SDS-PAGE and Western-blotting.

2.4. Synthesis of radiolabeled proteins and import into isolated mitochondria

Open reading frames of *COX26*, *COX13*, and *RCF1* were amplified using a forward primer containing the SP6 polymerase binding site and in the case of *COX26* the reverse primer encodes three additional methionine residues upstream of the stop codon. All constructs were in vitro transcribed using mMESSAGE mMACHINE SP6 Kit (Life Technologies). The obtained RNA was used for in vitro translation using the Flexi Rabbit Reticulocyte Lysate System (Promega) in the presence of [^{35}S]methionine. The open reading frame of *COX5a* cloned into the pTnT™ vector (Promega) was used for lysate production with TnT® Quick Coupled Transcription/Translation System (Promega). Radiolabeled proteins were imported into isolated mitochondria according to published procedures [34]. In brief, isolated mitochondria were incubated with radiolabeled precursor proteins at 25 °C in import buffer (3% BSA, 250 mM sucrose, 80 mM KCl, 5 mM $MgCl_2$, 2 mM KH_2PO_4, 5 mM methionine, 10 mM MOPS/KOH pH 7.2, 3 mM ATP, and 3 mM NADH). For assembly assays import buffer was supplemented with an ATP-regeneration system (8 mM creatine phosphate and 0.16 mg/ml creatine kinase). The import reactions were stopped on ice by dissipation of membrane potential with AVO mix (8 mM antimycin A, 1 mM valinomycin, and 10 mM oligomycin) and subjected to a proteinase K treatment. Mitochondria were analyzed by BN-PAGE and SDS-PAGE. Gels were dried and exposed on phosphorimager screens (GE Healthcare) for detection of radioactive signal by digital autoradiography.

2.5. IgG affinity chromatography

For complex isolation mitochondria from wild-type (WT) and ZZ tagged strains were solubilized on ice in solubilization buffer (20 mM Tris/HCl pH 7.4, 0.1 M NaCl, 5% glycerol, 0.5 mM EDTA, 2 mM phenylmethylsulfonyl fluoride (PMSF), 1% digitonin, or 0.6% dodecylmaltoside (DDM)) for 30 min. After a clarifying spin (15 min; 16,000 × *g*; 4 °C) samples were incubated with IgG Sepharose for 2 h at 4 °C with mild agitation. After extensive washing with solubilization buffer containing 0.3% digitonin or 0.6% DDM, samples were eluted directly with SDS loading buffer and subsequently analyzed by SDS-PAGE and Western-blotting.

2.6. Oxygen consumption measurements

High-resolution respirometry was assayed in isolated yeast mitochondria using Oxygraph-2 k (OROBOROS Instruments, Innsbruck, Austria) in standard configuration at 30 °C, 750 rpm stirrer speed, and two-point calibrations of the polarographic oxygen sensors. Oxygen consumption was measured in 2 ml chambers filled with respiratory media (70 mM sucrose, 220 mM mannitol, 1 mM EDTA, 5 mM $MgCl_2$, 2 mM HEPES, 10 mM KH_2PO_4 pH 7.4) in the presence of 1 mM NADH as a substrate and 1 mM ADP. Data analysis was performed with DatLab 4.

Table 1
Yeast strains used in this study.

Strain	Genotype	Reference
YPH499	*MATa, ade2-101, his3-Δ200, leu2-Δ1, ura3-52, trp1-Δ63, lys2-801*	[29]
Cox26^{GFP}	*MATa, ade2-101, his3-Δ200, leu2-Δ1, ura3-52, trp1-Δ63, lys2-801, cox26*::*cox26*-GFP-*KANMX4*	This study
Cox26^{FLAG}	*MATa, ade2-101, his3-Δ200, leu2-Δ1, ura3-52, trp1-Δ63, lys2-801, cox26*::*cox26*-FLAG-*HIS3MX6*	This study
Cox26^{ZZ}	*MATa, ade2-101, his3-Δ200, leu2-Δ1, ura3-52, trp1-Δ63, lys2-801, cox26*::*cox26*-TEV-ProA-7HIS-*HIS3MX6*	This study
Cox26^{BirA}	*MATa, ade2-101, his3-Δ200, leu2-Δ1, ura3-52, trp1-Δ63, lys2-801, cox26*::*cox26*-BirA-*HIS3MX6*	This study
*cox26*Δ	*MATa, ade2-101, his3-Δ200, leu2-Δ1, ura3-52, trp1-Δ63, lys2-801, cox26*::loxP	This study
Cox4^{ZZ}	*MATa, ade2-101, his3-Δ200, leu2-Δ1, ura3-52, trp1-Δ63, lys2-801, cox4*::*cox4*-TEV-ProA-7HIS-*HIS3MX6*	[26]
*cyt1*Δ	*MATa, ade2-101, his3-Δ200, leu2-Δ1, ura3-52, trp1-Δ63, lys2-801, cyt1*::*HISMX6*	[26]
*cox4*Δ	*MATa, ade2-101, his3- Δ200, leu2-Δ1, ura3-52, trp1-Δ63, lys2-801, cox4*::*HISMX6*	[32]

2.7. Mitochondrial enzyme activity measurements

Enzymatic activities were assayed spectrophotometrically essentially as described previously [26]. Malate dehydrogenase activity was determined by following the oxaloacetate-dependent oxidation of NADH at 340 nm in assay buffer (100 mM potassium phosphate buffer pH 7.4, 0.1 mM NADH, and 0.2 mM oxaloacetate). The extinction coefficient of NADH at 340 nm was 6.3 mM^{-1} cm^{-1}. NADH–cytochrome *c* reductase activity was measured in 40 mM potassium phosphate buffer pH 7.4, supplemented with 0.5 mM NADH and 0.02% bovine heart cytochrome *c* (Sigma-Aldrich) by following cytochrome *c* reduction at 550 nm. Prior to the measurement isolated mitochondria were treated with 10 mM KCN. For cytochrome *c* oxidase activity assay mitochondria were suspended in 40 mM potassium phosphate buffer pH 7.4 with 0.02% cytochrome *c* (reduced with sodium dithionite for oxidase activity) and cytochrome *c* oxidation was measured at 550 nm. Concentrations of reduced/oxidized cytochrome *c* were determined using the extinction coefficient at 550 nm of 21.84 mM^{-1} cm^{-1}.

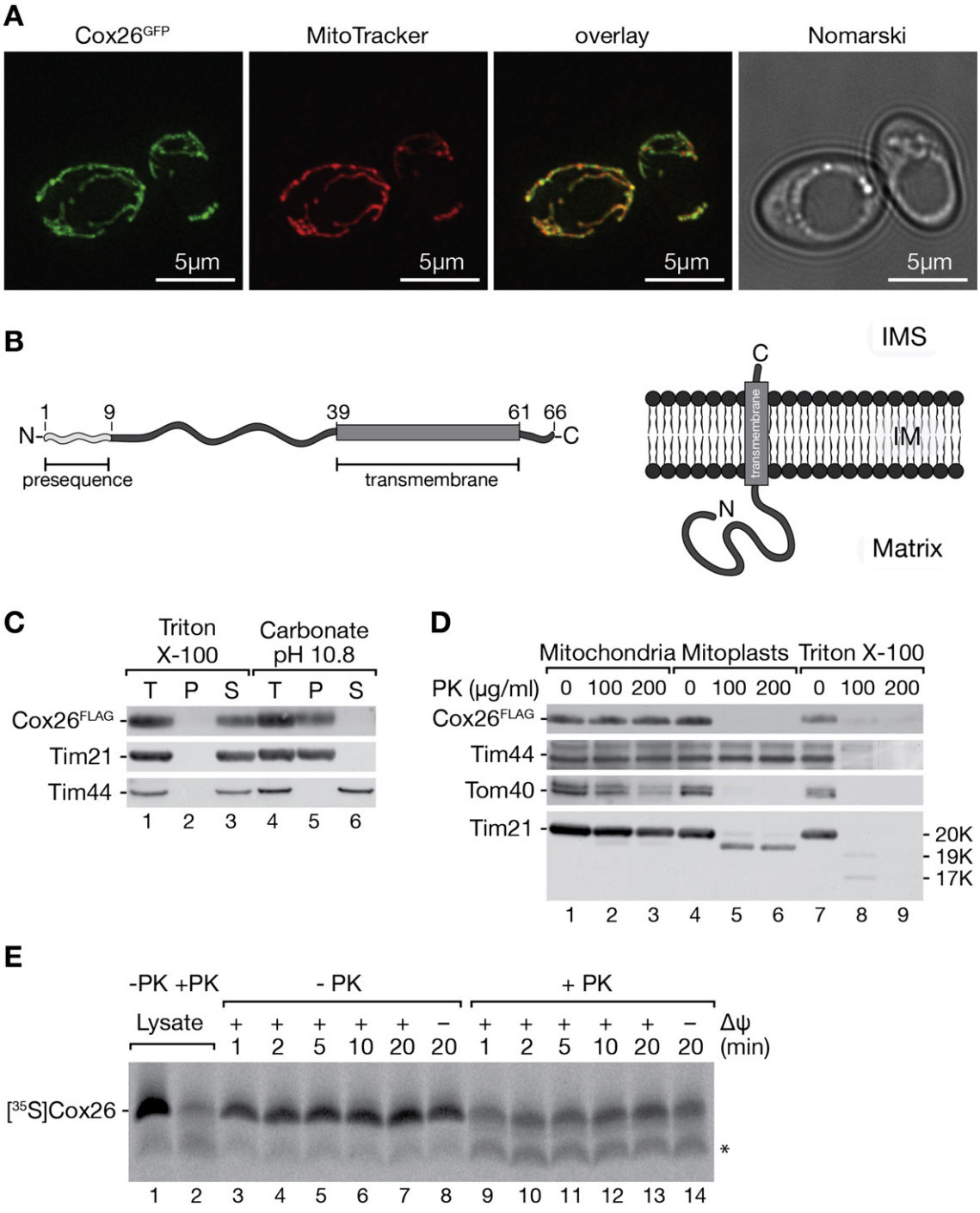

Fig. 1. Cox26 is a mitochondrial inner membrane protein (A) Yeast cells expressing $Cox26^{GFP}$ were grown in synthetic medium to mid-log phase and stained with MitoTracker Orange. Cells were analyzed by fluorescence microscopy. (B) Schematic representation of Cox26 protein; numbers indicate amino acid residues. (C) Membrane association of $Cox26^{FLAG}$ was assessed by carbonate extraction. Total, (T); pellet, (P); supernatant, (S). (D) Sub-mitochondrial localization of $Cox26^{FLAG}$. Indicated amounts of proteinase K (PK) were added to untreated, swollen, or Triton X-100 lysed mitochondria. (E) Radiolabeled Cox26 was imported into mitochondria for indicated times in the presence or absence of membrane potential (Δψ) and subjected to treatment with proteinase K (PK), where indicated. As a control 10% reticulocyte lysate containing radiolabeled Cox26 was applied. * marks a PK resistant fragment of the non-imported Cox26.

2.8. In-gel activity staining

In-gel activity staining of OXPHOS complexes was performed according to established protocols [35]. In brief, after separation of protein complexes by BN-PAGE, gel lanes were equilibrated in corresponding buffer for 15 min and incubated in staining solution at room temperature until color appeared. Cytochrome *c* oxidase equilibration buffer (50 mM potassium phosphate buffer pH 7.2) and staining solution (equilibration buffer with 0.5 mg/ml diaminobenzidine and 1 mg/ml bovine heart cytochrome *c* reduced with sodium dithionite); F_1F_o-ATPase equilibration buffer (35 mM Tris, 270 mM glycine, pH 8.3) and staining solution (equilibration buffer with 0.2% $Pb(NO_3)_2$, 8 mM ATP, 14 mM $MgSO_4$).

2.9. Measurements of mitochondrial ROS production

ROS levels were measured using H_2DFFDA (Invitrogen), a molecular probe that becomes fluorescent upon oxidation by ROS, as previously described [29]. Change in fluorescence [λ_{ex} = 495 nm, λ_{em} = 525 nm] of 200 μM H_2DDFDA in assay buffer (20 mM Tris pH 7.4, 150 mM NaCl, 0.1% Triton X-100) supplemented with isolated yeast mitochondria was recorded with HITACHI F-7000 fluorescence spectrophotometer.

2.10. Miscellaneous

Standard techniques were used for SDS-PAGE and Western-blotting to polyvinylidene fluoride (PVDF) membranes. For detection and visualization of antibody-protein complexes, peroxidase-conjugated goat anti-rabbit and anti-mouse IgG (Jackson ImmunoResearch) and enhanced chemiluminescence reagent (GE Healthcare) were used. ZZ tag was visualized with peroxidase-anti peroxidase soluble complex antibody (Sigma-Aldrich). BN-PAGE protocols followed published procedures [36]. In brief, mitochondria were solubilized in solubilization buffer (20 mM Tris/HCl pH 7.4, 0.1 mM EDTA, 0.1 M NaCl, 10% glycerol, 2 mM PMSF, 1% digitonin, or 0.6% DDM) for 15 min at 4 °C. After clarifying spin (15 min; 16,000 g; 4 °C) samples were mixed with 10× loading dye (5% Coomassie G-250, 0.5 M 6-amino-hexanoic acid, and 0.1 M Bis-Tris, pH 7.0), and separated on a 4–13% native polyacrylamide gradient gel.

3. Results and discussion

3.1. Cox26 is a mitochondrial inner membrane protein

Mitochondrial respiratory chain complexes form supercomplexes to promote efficient electron transport and limit oxidative damage [17,20–23]. In *S. cerevisiae* two types of supercomplexes are present, a dimer of

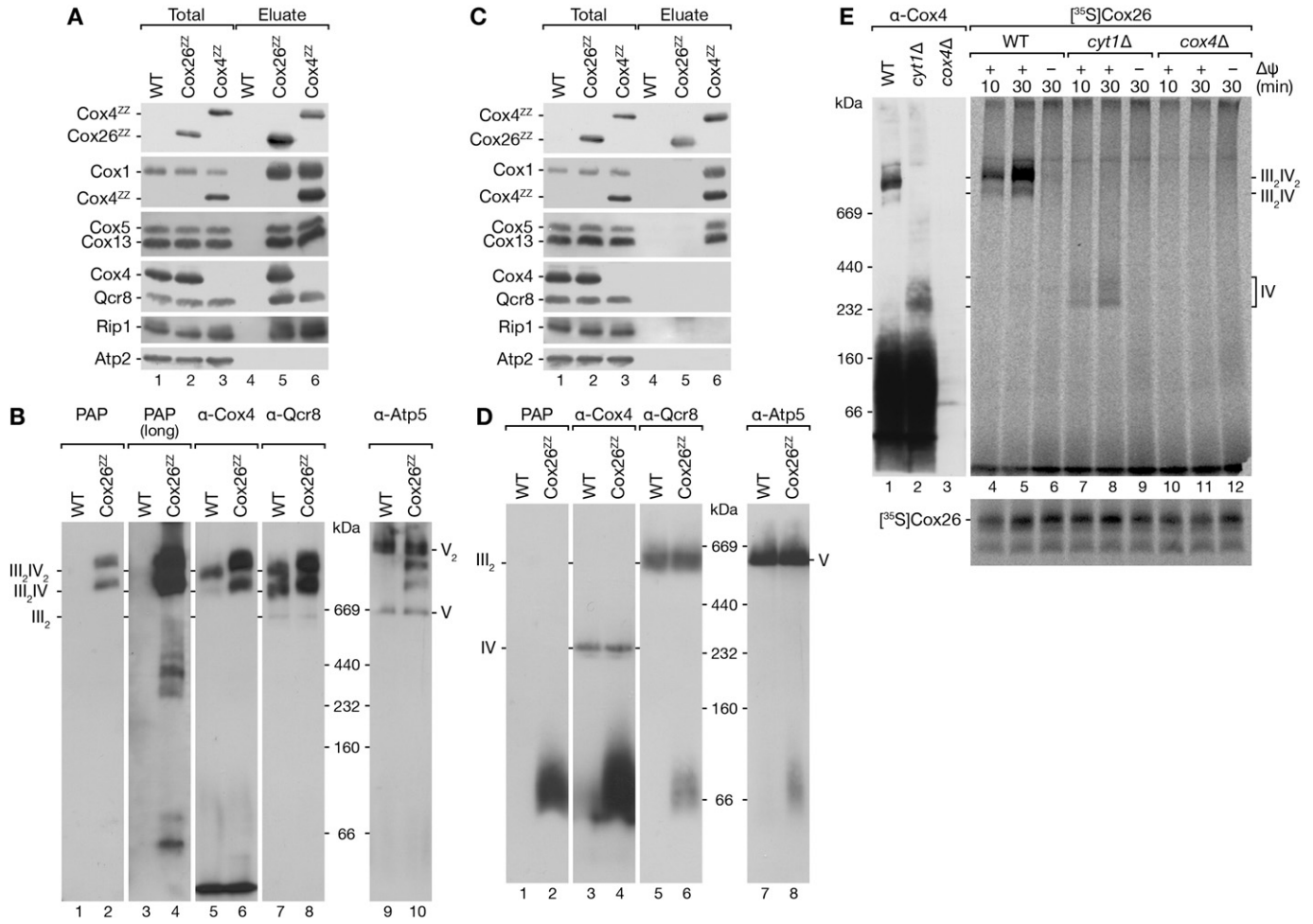

Fig. 2. Cox26 is a component of the cytochrome *c* oxidase (A) $Cox26^{ZZ}$ and $Cox4^{ZZ}$ complexes were isolated from digitonin-solubilized mitochondria via IgG chromatography and analyzed by Western-blotting. Total, 10%; eluate, 100%. (B) Wild-type (WT) and $Cox26^{ZZ}$ mitochondria were lysed in digitonin buffer, subjected to BN-PAGE, and analyzed by Western-blotting. PAP — peroxidase anti-peroxidase. (C)–(D) As in (A) and (B), but solubilized in DDM. (E) Radiolabeled Cox26 was imported into wild-type (WT), *cyt1*Δ, and *cox4*Δ mitochondria in the presence or absence of a membrane potential (Δψ) for indicated times. Samples were treated with proteinase K (PK), solubilized in 1% digitonin buffer, and analyzed by BN-PAGE and digital autoradiography. For comparison, solubilized mitochondria from corresponding strains were analyzed by BN-PAGE, followed by Western-blotting.

complex III (cytochrome *c* reductase) bound to one or two copies of complex IV (cytochrome *c* oxidase — COX). Extensive analyses have been carried out to define the composition of these assemblies. Several new components of yeast respirasomes have been identified and analyzed recently [26–28]. An uncharacterized protein YDR119W-A was initially seen to co-migrate with supercomplexes in crude mitochondrial extracts [37]. We found YDR119W-A by mass spectrometry in which it copurifies with respirasomes isolated by a tagged complex III subunit [26]. However, the association of YDR119W-A with respiratory chain supercomplexes was not confirmed, nor has the function of the protein been assessed.

To address an exclusive mitochondrial localization of YDR119W-A, from now on termed Cox26, within the cell, we expressed a $Cox26^{GFP}$ fusion from the endogenous chromosomal locus. Fluorescence microscopy analysis of living cells expressing $Cox26^{GFP}$ showed co-localization of the GFP signal with mitochondria visualized by MitoTracker staining. (Fig. 1A). This indicated that Cox26 resides exclusively in mitochondria. For further analysis of the Cox26 protein, we generated yeast strains with a C-terminal FLAG or ZZ tag integrated into the *COX26* locus. The primary sequence of Cox26 contains one predicted transmembrane span (Fig. 1B). In order to test membrane association of Cox26 we isolated mitochondria from the $Cox26^{FLAG}$-expressing cells and subjected them to carbonate extraction. $Cox26^{FLAG}$ was resistant to alkaline treatment at pH 10.8 and remained in the sediment fraction after centrifugation together with the integral membrane protein Tim21, while the peripheral membrane protein Tim44 was released into the supernatant (Fig. 1C). To determine the submitochondrial localization of Cox26, we performed protease protection experiments. The C-terminally FLAG tagged Cox26 remained stable in intact mitochondria upon protease treatment but became accessible in mitoplasts after osmotic disruption of the mitochondrial outer membrane (Fig. 1D). We concluded that Cox26 was an integral membrane protein of the mitochondrial inner membrane and exposed its small C-terminus into the intermembrane space (Fig. 1B). To assess mitochondrial import of Cox26, we synthesized the protein in vitro using rabbit reticulocyte lysate supplemented with [^{35}S]methionine

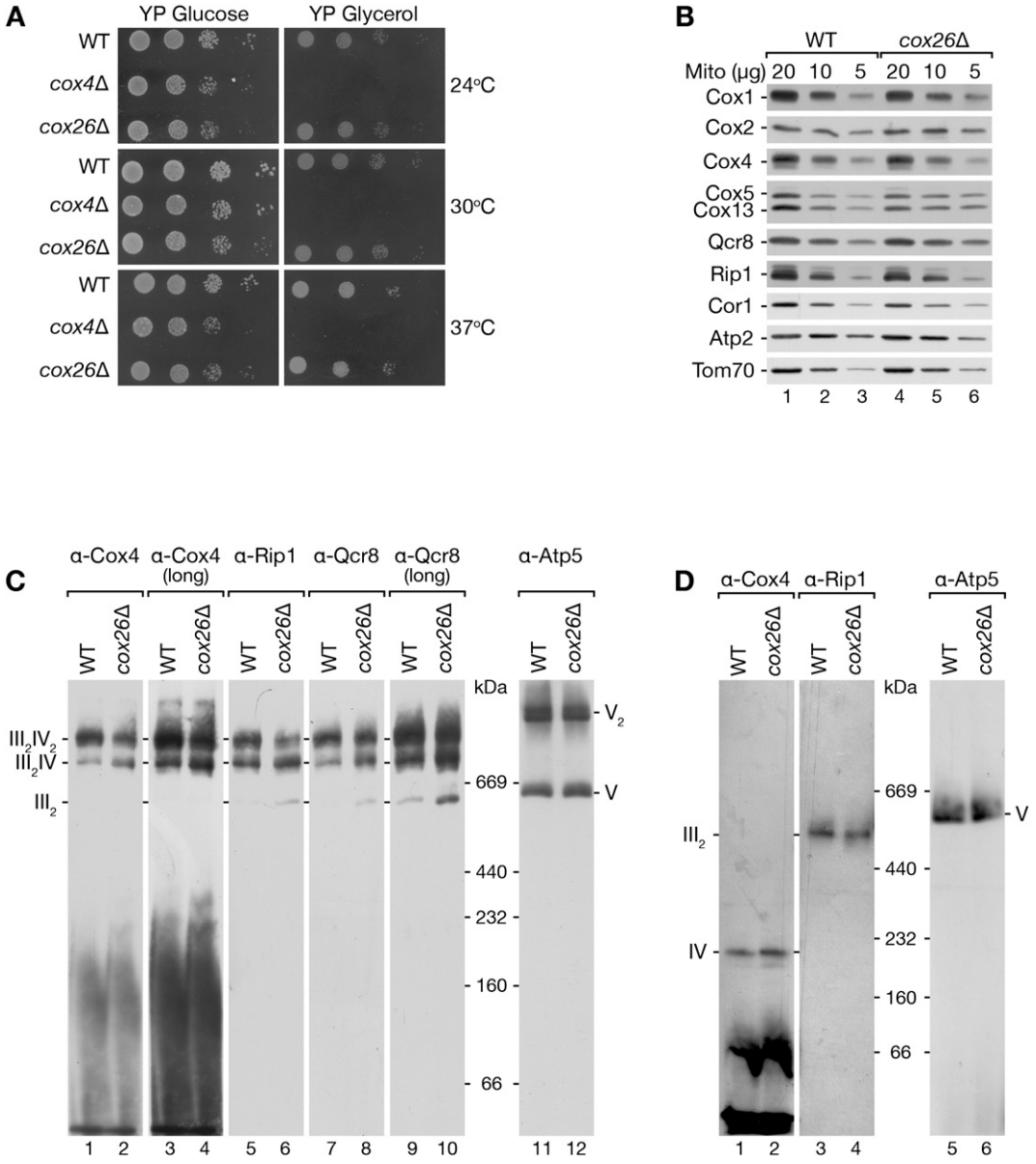

Fig. 3. Cox26 deletion leads to supercomplexes re-arrangement (A) Wild-type (WT), *cox4*Δ, and *cox26*Δ yeast cells were spotted in serial 10-fold dilutions on YP-glucose or YP-glycerol plates and grown at indicated temperatures for 2–5 days. (B) Isolated wild-type (WT) and *cox26*Δ mitochondria were subjected to SDS-PAGE and analyzed by Western-blotting. (C)–(D) Wild-type (WT) and *cox26*Δ mitochondria were lysed in 1% digitonin (C) or 0.6% DDM (D) buffer, subjected to BN-PAGE, and analyzed by Western-blotting.

for radioactive labeling. In addition to the single initial methionine of the protein we added three methionine residues to the C-terminus of Cox26 for better detection. After the import reaction, we found that Cox26 was transported to a protease-protected location within mitochondria even upon dissipation of the membrane potential ($\Delta\psi$). In addition, no processing of Cox26 to a faster migrating mature form was observed (Fig. 1E). To assess if a very short cleaveable presequence was present in Cox26 that was processed in vivo but was not resolved by SDS-PAGE, we isolated Cox26^{ZZ} from Triton X-100 solubilized mitochondria via IgG affinity chromatography. After removing the tag by TEV protease cleavage, the purified protein was subjected to SDS-PAGE and transferred to a nitrocellulose membrane. Following Coomassie staining the membrane piece containing Cox26 was excised, dissolved in DMSO and subjected to Edman sequencing to determine the N-terminal protein sequence. These analyses allowed us to assign the N-terminus of the authentic Cox26. Cox26 is processed by removal of the first eight amino acids of the protein leading to a mature Cox26 starting with serine number 9 (Fig. 1B).

3.2. Cox26 associates with respiratory chain supercomplexes via cytochrome c oxidase

To address if Cox26 was indeed a supercomplex-associated protein, we purified Cox26^{ZZ} together with its interaction partners from digitonin-solubilized mitochondria by IgG affinity chromatography. Cox4^{ZZ} was used as a positive control to pull down respiratory chain complexes. Eluates were analyzed by SDS-PAGE and Western-blotting. Cox26^{ZZ} co-isolated the tested components of complex IV (Cox1, Cox4, Cox5, Cox13) and complex III (Qcr8, Rip1) in amounts comparable to Cox4^{ZZ}, thus confirming Cox26 association with respirasomes (Fig. 2A).

To further support this finding, we analyzed digitonin-solubilized wild-type and Cox26^{ZZ} mitochondria by BN-PAGE and Western-

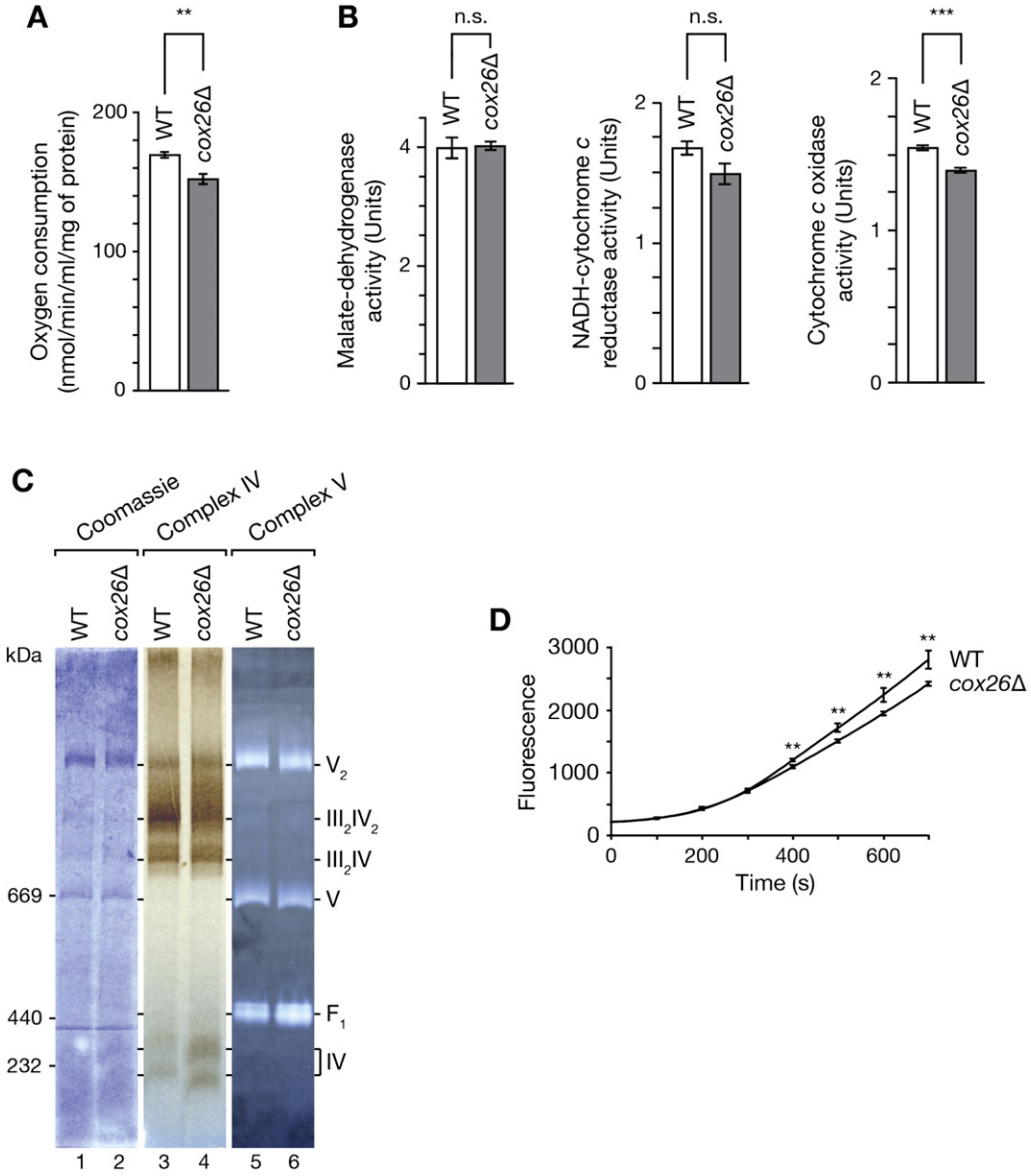

Fig. 4. Respiratory chain activity in the absence of Cox26 (A) Oxygen consumption rates of wild-type (WT) and *cox26*Δ mitochondria were determined by oxygraph measurement (mean of n = 4 ± SEM). (B) Mitochondrial enzyme activity assays of NADH-cytochrome *c* reductase, cytochrome *c* oxidase, and malate-dehydrogenase (mean of n = 5 ± SEM). (C) Digitonin-solubilized mitochondria from wild-type (WT) and *cox26*Δ cells were analyzed by BN-PAGE followed by Coomassie staining, cytochrome *c* oxidase (complex IV) or F_1F_o-ATPase (complex V) in-gel activity staining (D) Mitochondrial ROS production in wild-type (WT) and *cox26*Δ strains (mean of n = 4 ± SEM). Significance for A, B and D was calculated using Student's t-test. Abbreviations: n.s. = not significant, ** = $P < 0.01$, *** = $P < 0.0001$.

blotting. Cox26^{ZZ} was present in two high molecular weight assemblies that co-migrated with respiratory chain supercomplexes decorated with antibodies against subunits of complex III (Qcr8) and complex IV (Cox4) (Fig. 2B). Moreover, supercomplexes in Cox26^{ZZ} mitochondria appeared shifted in size compared to the wild-type. This shift is likely due to the extra mass added by the ZZ tag on Cox26. Compared to complex IV-containing supercomplexes the dimer of complex III was not shifted in size by Cox26^{ZZ}, therefore we concluded that Cox26 was associated with supercomplexes through complex IV. After long exposure of the blots, we detected Cox26^{ZZ} also in several complexes between 230 and 440 kDa that likely correspond to monomeric forms of complex IV.

To assess if Cox26 was indeed a complex IV component, we repeated Cox26^{ZZ} isolation from dodecylmaltoside (DDM)-solubilized mitochondria. Upon DDM solubilization supercomplexes dissociate into complex IV monomers and complex III dimers [16]. However, under these conditions Cox26^{ZZ} did not co-isolate components of complex IV in contrast to Cox4^{ZZ}, which was still associated with the cytochrome *c* oxidase (Fig. 2C). Similarly, in BN-PAGE analysis of DDM-solubilized mitochondria Cox26^{ZZ} was not present in high molecular weight assemblies (Fig. 2D). This observation suggested that Cox26 dissociates from supercomplexes under these solubilization conditions. To overcome this problem, we imported radiolabeled Cox26 into wild-

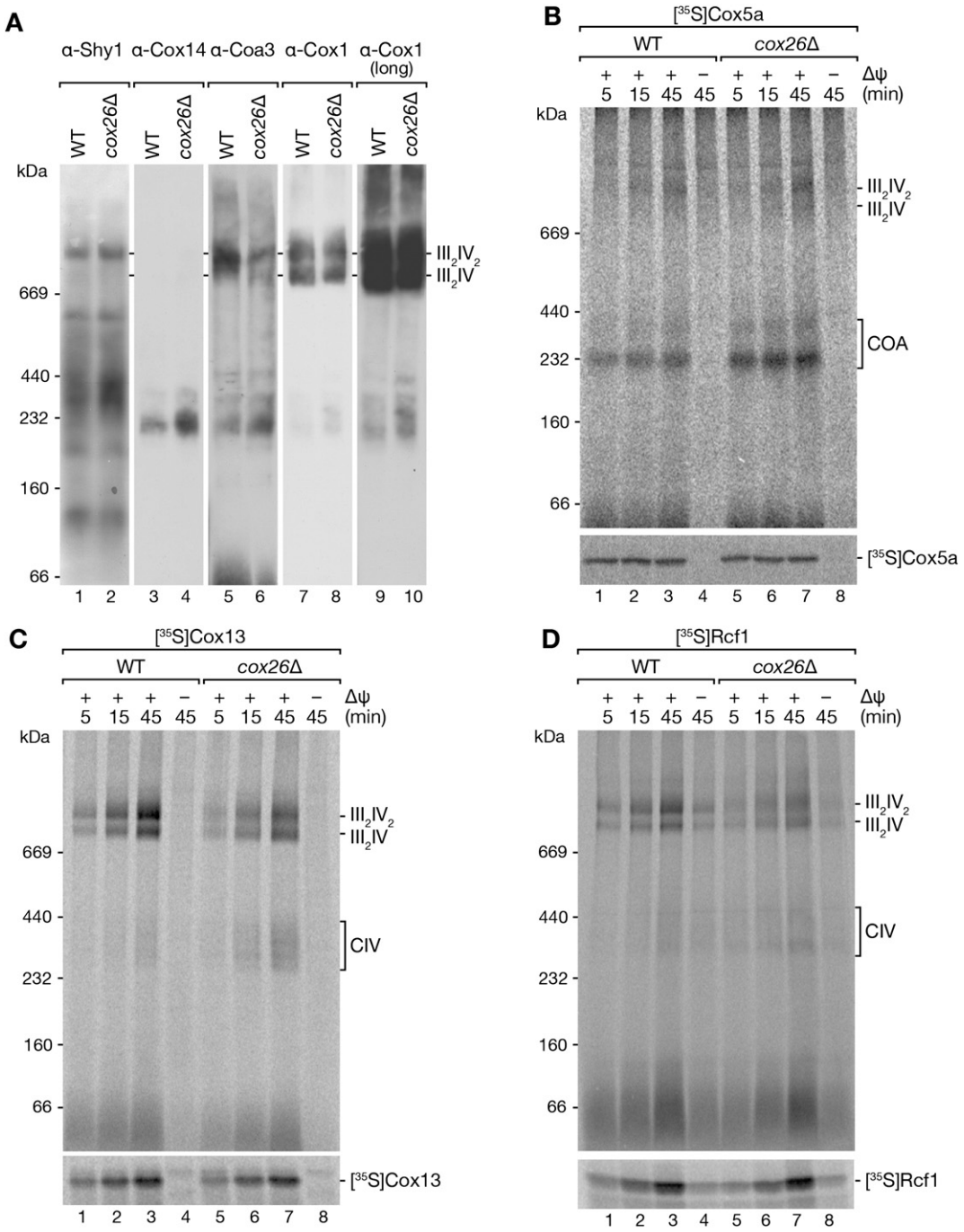

Fig. 5. Cox26 deficient mitochondria accumulate cytochrome *c* oxidase assembly intermediates (A) Wild-type (WT) and *cox26*Δ mitochondria were lysed in 1% digitonin buffer, subjected to BN-PAGE, and analyzed by Western-blotting. (B)–(D) Radiolabeled Cox5a (B), Cox13 (C), and Rcf1 (D) were imported into purified wild-type (WT) and *cox26*Δ mitochondria in the presence or absence of Δψ for indicated times and treated with proteinase K (PK). Samples were lysed in 1% digitonin buffer, analyzed by BN-PAGE, SDS-PAGE, and digital autoradiography. COA — cytochrome *c* oxidase assembly intermediate.

type and mutant mitochondria deficient in complex III (*cyt1*Δ) or complex IV (*cox4*Δ) formation. After import, we analyzed protein complexes by BN-PAGE. In the wild-type mitochondria, Cox26 assembled predominantly into two protein complexes corresponding to the supercomplexes visualized with the Cox4 antibody (Fig. 2E). Cox26 was imported with similar efficiency into wild-type and mutant mitochondria (Fig. 2E, lower panel). However, when Cox26 assembly was analyzed by BN-PAGE, we could detect two complexes corresponding to the monomeric forms of complex IV in *cyt1*Δ mitochondria, in contrast to the *cox4*Δ mitochondria, where Cox26 formed no high molecular weight assemblies. Even in the absence of Rcf1, a factor involved in complex III complex IV supercomplex formation, radiolabeled Cox26 remains associated with complex IV (Fig. S1A). Accordingly, we conclude that Cox26 is a constituent of the cytochrome *c* oxidase. Taking the capability of Cox26^{ZZ} to shift the entire cytochrome *c* oxidase-containing complexes in size into consideration, we further conclude that Cox26 is a stoichiometric subunit of complex IV. The dissociation from complex IV upon DDM treatment most likely reflects a weak association with the complex under these conditions.

3.3. Deletion of COX26 affects assembly of active cytochrome c oxidase into supercomplexes

To assess the function of Cox26 with regard to respiratory chain activity, we generated a *cox26*Δ mutant. Cox26 was dispensable for yeast growth on fermentable and non-fermentable carbon sources at various temperatures in contrast to the tested respiratory-deficient mutant *cox4*Δ (Fig. 3A). We compared the steady-state levels of several mitochondrial proteins in wild-type (WT) and *cox26*Δ mitochondria by Western-blotting. However, no differences for any of the tested proteins was detected (Fig. 3B). Since Cox26 associates with supercomplexes, we speculated that the absence of Cox26 could affect supercomplex organization. Hence we performed BN-PAGE analysis of digitonin-solubilized *cox26*Δ mitochondria. Mutant mitochondria displayed reduced amounts of III_2IV_2 complexes and increased levels of III_2IV. We quantified the amount of the III_2IV supercomplex detected with Cox4 and Rip1 from different experiments. Compared to the wild-type control, on average we observed an increase to 162% (Cox4) or 142% (Rip1) in *cox26*Δ mutant mitochondria. Concomitantly, free complex III_2 was apparent in the mutant mitochondria sample (Fig. 3C). This defect could reflect reduced stability of the III_2IV_2 complexes in the absence of Cox26 or occur due to reduced levels of complex IV. To address if the amount of individual respiratory chain complexes were altered in *cox26*Δ mitochondria, we solubilized mitochondria in DDM-containing buffer and separated complexes by BN-PAGE. Compared to the wild-type, we did not observe any differences in complex IV or complex III levels in *cox26*Δ mitochondria (Fig. 3D). Accordingly, supercomplexes are specifically affected by the absence of Cox26.

Improper supercomplex formation has been reported to lead to respiratory defects [29]. Therefore, we assayed O_2 consumption in *cox26*Δ mitochondria with an OROBOROS-2k oxygraph. *cox26*Δ mutant mitochondria displayed a reproducible mild reduction of the oxygen consumption rate, to approximately 90% of the wild-type (Fig. 4A). Similarly, enzyme activity assays demonstrated that *cox26*Δ cells were only slightly defective in complex III and IV activity (Fig. 4B). In contrast, malate dehydrogenase activity was not affected. To visualize active respiratory complexes we performed in-gel activity staining. Digitonin-solubilized WT and *cox26*Δ mitochondria were subjected to BN-PAGE and the corresponding gel strips were analyzed for complex activity or stained with Coomassie to assess protein levels. Complex IV staining showed reduced activity of the III_2IV_2 supercomplex in the mutant (Fig. 4C), which correlates with the lower supercomplex amount (as seen in Fig. 3C). Simultaneously, we detected more of the active complex IV monomer in the *cox26*Δ sample. The complexes also appeared to be shifted in size, possibly due to the loss of the cytochrome *c* oxidase subunit (Fig. 4C, lane 3 vs. 4). In contrast, the F_1F_o-ATPase activity remained unaltered. Since inefficient supercomplex formation may lead to the production of reactive oxygen species (ROS) we addressed ROS generation in mutant mitochondria [29]. We detected a 10% reduction of mitochondrial ROS production in *cox26*Δ compared to wild-type (Fig. 4D).

Since we observed a reduction of III_2IV_2 supercomplex formation in the absence of Cox26 (Figs. 3C and 4C), we analyzed if this defect was due to complex dissociation or a defect in the assembly process. To test this, we checked the levels of cytochrome *c* oxidase assembly factors, such as Shy1, Cox14, and Coa3 by BN-PAGE analysis [38,39]. While the steady-state levels of Shy1, Coa1 and Cox14 were not altered (Fig. S1B) in *cox26*Δ mitochondria, we observed an accumulation of complex IV assembly intermediates (Fig. 5A). A similar phenotype was observed upon import of Cox5a, an early assembling subunit [8], into wild-type and *cox26*Δ mitochondria. BN-PAGE analysis combined with digital autoradiography revealed higher levels of complex IV assembly intermediates in Cox26-deficient mitochondria (Fig. 5B). This observation indicates an alteration in the assembly process, which in turn may lead to a decrease in supercomplex formation. To further test this, we monitored assembly of the late complex IV subunits, such as Cox13 and Rcf1. Radiolabeled proteins were imported into wild-type and *cox26*Δ mitochondria and complexes were separated by BN-PAGE. Both Cox13 and Rcf1 were incorporated into supercomplexes in wild-type mitochondria. In the mutant, incorporation efficiency was decreased even considering the changed ratio between supercomplexes observed at steady state level. These analyses support the conclusion that the assembly efficiency of Cox13 and Rcf1 is decreased in the absence of Cox26 (Fig. 5C and D).

4. Conclusions

The cytochrome *c* oxidase consists of conserved structural subunits forming the enzymatic core [8,9,40]. In higher eukaryotes tissue-specific versions of some subunits have been reported, indicating that the function of the respiratory chain has to be adapted to cellular demands in a cell type and metabolic context-specific manner [41–43]. In addition to structural subunits required for enzymatic function, supplementary factors engage with complex IV e.g. to modulate its association with complex III into respirasomes [26–28,44]. It is unclear if the specific mechanisms of respiratory chain supercomplex formation are similar between yeast and human and if they involve similar components. Rcf1 has been described as an oligomerization factor for complex III and complex IV supercomplex organization. Recent studies suggest novel factors that are involved in the formation of human and mouse supercomplexes that assemble from single enzyme complexes (I, III and IV) [45]. It is likely that besides Rcf1 additional factors participate in respirasome formation in yeast. Here we identified Cox26 as a new subunit of complex IV that is not conserved in higher eucaryotes. Based on our analyses, we propose that Cox26 is a stoichiometric subunit of complex IV. While a loss of Cox26 only mildly affects complex IV under experimental conditions, we find that the protein contributes to proper enzyme function and efficient incorporation of the complex into respiratory chain supercomplexes.

Supplementary data to this article can be found online at http://dx.doi.org/10.1016/j.bbamcr.2016.04.007.

Transparency document

The Transparency document associated with this article can be found in online version.

Acknowledgments

We thank B. Schwappach and S. Jakobs for their helpful discussions. This work was supported by the Deutsche Forschungsgemeinschaft

(MD & PR), the Ph.D. program "Molecular Biology" – International Max Planck Research School and the Göttingen Graduate School for Neurosciences and Molecular Biosciences (GGNB) (DFG grant GSC 226/1) at the Georg August University Göttingen (ML), Boehringer Ingelheim Fonds (ML), and the Max Planck Society (PR).

References

[1] T. Yamashita, E. Nakamaru-Ogiso, H. Miyoshi, A. Matsuno-Yagi, T. Yagi, Roles of bound quinone in the single subunit NADH-quinone oxidoreductase (Ndi1) from *Saccharomyces cerevisiae*, J. Biol. Chem. 282 (2007) 6012–6020, http://dx.doi.org/10.1074/jbc.M610646200.

[2] J. Rutter, D.R. Winge, J.D. Schiffman, Succinate dehydrogenase — assembly, regulation and role in human disease, Mitochondrion 10 (2010) 393–401, http://dx.doi.org/10.1016/j.mito.2010.03.001.

[3] V. Zara, L. Conte, B.L. Trumpower, Biogenesis of the yeast cytochrome bc1 complex, Biochim. Biophys. Acta 1793 (2009) 89–96, http://dx.doi.org/10.1016/j.bbamcr.2008.04.011.

[4] A. Maréchal, B. Meunier, D. Lee, C. Orengo, P.R. Rich, Yeast cytochrome c oxidase: a model system to study mitochondrial forms of the haem-copper oxidase superfamily, Biochim. Biophys. Acta 1817 (2012) 620–628, http://dx.doi.org/10.1016/j.bbabio.2011.08.011.

[5] K.M. Davies, C. Anselmi, I. Wittig, J.D. Faraldo-Gómez, W. Kühlbrandt, Structure of the yeast F_1F_o-ATP synthase dimer and its role in shaping the mitochondrial cristae, Proc. Natl. Acad. Sci. U. S. A. 109 (2012) 13602–13607, http://dx.doi.org/10.1073/pnas.1204593109.

[6] M. Ott, J.M. Herrmann, Co-translational membrane insertion of mitochondrially encoded proteins, Biochim. Biophys. Acta 1803 (2010) 767–775, http://dx.doi.org/10.1016/j.bbamcr.2009.11.010.

[7] E. Fernández-Vizarra, M. Zeviani, Nuclear gene mutations as the cause of mitochondrial complex III deficiency, Front. Genet. 6 (2015) 134, http://dx.doi.org/10.3389/fgene.2015.00134.

[8] D.U. Mick, T.D. Fox, P. Rehling, Inventory control: cytochrome c oxidase assembly regulates mitochondrial translation, Nat. Rev. Mol. Cell Biol. 12 (2011) 14–20, http://dx.doi.org/10.1038/nrm3029.

[9] I.C. Soto, F. Fontanesi, J. Liu, A. Barrientos, Biogenesis and assembly of eukaryotic cytochrome c oxidase catalytic core, Biochim. Biophys. Acta 1817 (2012) 883–897, http://dx.doi.org/10.1016/j.bbabio.2011.09.005.

[10] G.P. McStay, C.H. Su, A. Tzagoloff, Modular assembly of yeast cytochrome oxidase, Mol. Biol. Cell 24 (2013) 440–452, http://dx.doi.org/10.1091/mbc.E12-10-0749.

[11] J.M. Herrmann, M.W. Woellhaf, N. Bonnefoy, Control of protein synthesis in yeast mitochondria: the concept of translational activators, Biochim. Biophys. Acta 1833 (2013) 286–294, http://dx.doi.org/10.1016/j.bbamcr.2012.03.007.

[12] N. Bonnefoy, H.L. Fiumera, G. Dujardin, T.D. Fox, Roles of Oxa1-related inner-membrane translocases in assembly of respiratory chain complexes, Biochim. Biophys. Acta 1793 (2009) 60–70, http://dx.doi.org/10.1016/j.bbamcr.2008.05.004.

[13] M. Keil, B. Bareth, M.W. Woellhaf, V. Peleh, M. Prestele, P. Rehling, et al., Oxa1-ribosome complexes coordinate the assembly of cytochrome C oxidase in mitochondria, J. Biol. Chem. 287 (2012) 34484–34493, http://dx.doi.org/10.1074/jbc.M112.382630.

[14] H.J. Kim, O. Khalimonchuk, P.M. Smith, D.R. Winge, Structure, function, and assembly of heme centers in mitochondrial respiratory complexes, Biochim. Biophys. Acta 1823 (2012) 1604–1616, http://dx.doi.org/10.1016/j.bbamcr.2012.04.008.

[15] I. Arnold, K. Pfeiffer, W. Neupert, R.A. Stuart, H. Schägger, Yeast mitochondrial F_1F_o-ATP synthase exists as a dimer: identification of three dimer-specific subunits, EMBO J. 17 (1998) 7170–7178, http://dx.doi.org/10.1093/emboj/17.24.7170.

[16] H. Schägger, K. Pfeiffer, Supercomplexes in the respiratory chains of yeast and mammalian mitochondria, EMBO J. 19 (2000) 1777–1783, http://dx.doi.org/10.1093/emboj/19.8.1777.

[17] G. Lenaz, M.L. Genova, Structure and organization of mitochondrial respiratory complexes: a new understanding of an old subject, Antioxid. Redox Signal. 12 (2010) 961–1008, http://dx.doi.org/10.1089/ars.2009.2704.

[18] N.V. Dudkina, R. Kouril, K. Peters, H.-P. Braun, E.J. Boekema, Structure and function of mitochondrial supercomplexes, Biochim. Biophys. Acta 1797 (2010) 664–670, http://dx.doi.org/10.1016/j.bbabio.2009.12.013.

[19] E. Mileykovskaya, P.A. Penczek, J. Fang, V.K.P.S. Mallampalli, G.C. Sparagna, W. Dowhan, Arrangement of the respiratory chain complexes in *Saccharomyces cerevisiae* supercomplex III2IV2 revealed by single particle cryo-electron microscopy, J. Biol. Chem. 287 (2012) 23095–23103, http://dx.doi.org/10.1074/jbc.M112.367888.

[20] T. Althoff, D.J. Mills, J.-L. Popot, W. Kühlbrandt, Arrangement of electron transport chain components in bovine mitochondrial supercomplex I1III2IV1, EMBO J. 30 (2011) 4652–4664, http://dx.doi.org/10.1038/emboj.2011.324.

[21] A. Ghelli, C.V. Tropeano, M.A. Calvaruso, A. Marchesini, L. Iommarini, A.M. Porcelli, et al., The cytochrome b p.278Y>C mutation causative of a multisystem disorder enhances superoxide production and alters supramolecular interactions of respiratory chain complexes, Hum. Mol. Genet. 22 (2013) 2141–2151, http://dx.doi.org/10.1093/hmg/ddt067.

[22] E. Maranzana, G. Barbero, A.I. Falasca, G. Lenaz, M.L. Genova, Mitochondrial respiratory supercomplex association limits production of reactive oxygen species from complex I, Antioxid. Redox Signal. 19 (2013) 1469–1480, http://dx.doi.org/10.1089/ars.2012.4845.

[23] M.L. Genova, G. Lenaz, Functional role of mitochondrial respiratory supercomplexes, Biochim. Biophys. Acta 1837 (2014) 427–443, http://dx.doi.org/10.1016/j.bbabio.2013.11.002.

[24] M. Zhang, E. Mileykovskaya, W. Dowhan, Cardiolipin is essential for organization of complexes III and IV into a supercomplex in intact yeast mitochondria, J. Biol. Chem. 280 (2005) 29403–29408, http://dx.doi.org/10.1074/jbc.M504955200.

[25] K. Brandner, D.U. Mick, A.E. Frazier, R.D. Taylor, C. Meisinger, P. Rehling, Taz1, an outer mitochondrial membrane protein, affects stability and assembly of inner membrane protein complexes: implications for Barth syndrome, Mol. Biol. Cell 16 (2005) 5202–5214, http://dx.doi.org/10.1091/mbc.E05-03-0256.

[26] M. Vukotic, S. Oeljeklaus, S. Wiese, F.N. Vögtle, C. Meisinger, H.E. Meyer, et al., Rcf1 mediates cytochrome oxidase assembly and respirasome formation, revealing heterogeneity of the enzyme complex, Cell Metab. 15 (2012) 336–347, http://dx.doi.org/10.1016/j.cmet.2012.01.016.

[27] Y.-C. Chen, E.B. Taylor, N. Dephoure, J.-M. Heo, A. Tonhato, I. Papandreou, et al., Identification of a protein mediating respiratory supercomplex stability, Cell Metab. 15 (2012) 348–360, http://dx.doi.org/10.1016/j.cmet.2012.02.006.

[28] V. Strogolova, A. Furness, M. Robb-McGrath, J. Garlich, R.A. Stuart, Rcf1 and Rcf2, members of the hypoxia-induced gene 1 protein family, are critical components of the mitochondrial cytochrome bc1-cytochrome c oxidase supercomplex, Mol. Cell. Biol. 32 (2012) 1363–1373, http://dx.doi.org/10.1128/MCB.06369-11.

[29] R.S. Sikorski, P. Hieter, A system of shuttle vectors and yeast host strains designed for efficient manipulation of DNA in *Saccharomyces cerevisiae*, Genetics 122 (1989) 19–27.

[30] M. Knop, K. Siegers, G. Pereira, W. Zachariae, B. Winsor, K. Nasmyth, et al., Epitope tagging of yeast genes using a PCR-based strategy: more tags and improved practical routines, Yeast 15 (1999) 963–972, http://dx.doi.org/10.1002/(SICI)1097-0061(199907)15:10B<963::AID-YEA399>3.0.CO;2-W.

[31] M.S. Longtine, A. McKenzie, D.J. Demarini, N.G. Shah, A. Wach, A. Brachat, et al., Additional modules for versatile and economical PCR-based gene deletion and modification in *Saccharomyces cerevisiae*, Yeast 14 (1998) 953–961, http://dx.doi.org/10.1002/(SICI)1097-0061(199807)14:10<953::AID-YEA293>3.0.CO;2-U.

[32] A.E. Frazier, R.D. Taylor, D.U. Mick, B. Warscheid, N. Stoepel, H.E. Meyer, et al., Mdm38 interacts with ribosomes and is a component of the mitochondrial protein export machinery, J. Cell Biol. 172 (2006) 553–564, http://dx.doi.org/10.1083/jcb.200505060.

[33] C. Meisinger, N. Pfanner, K.N. Truscott, Isolation of yeast mitochondria, Methods Mol. Biol. 313 (2006) 33–39, http://dx.doi.org/10.1385/1-59259-958-3:033.

[34] N. Wiedemann, N. Pfanner, P. Rehling, Import of precursor proteins into isolated yeast mitochondria, Methods Mol. Biol. 313 (2006) 373–383, http://dx.doi.org/10.1385/1-59259-958-3:373.

[35] I. Wittig, H. Schägger, Advantages and limitations of clear-native PAGE, Proteomics 5 (2005) 4338–4346, http://dx.doi.org/10.1002/pmic.200500081.

[36] P.J. Dekker, F. Martin, A.C. Maarse, U. Bömer, H. Müller, B. Guiard, et al., The Tim core complex defines the number of mitochondrial translocation contact sites and can hold arrested preproteins in the absence of matrix Hsp70-Tim44, EMBO J. 16 (1997) 5408–5419, http://dx.doi.org/10.1093/emboj/16.17.5408.

[37] A.O. Helbig, M.J.L. de Groot, R.A. van Gestel, S. Mohammed, E.A.F. de Hulster, M.A.H. Luttik, et al., A three-way proteomics strategy allows differential analysis of yeast mitochondrial membrane protein complexes under anaerobic and aerobic conditions, Proteomics 9 (2009) 4787–4798, http://dx.doi.org/10.1002/pmic.200800951.

[38] D.U. Mick, K. Wagner, M. van der Laan, A.E. Frazier, I. Perschil, M. Pawlas, et al., Shy1 couples Cox1 translational regulation to cytochrome c oxidase assembly, EMBO J. 26 (2007) 4347–4358, http://dx.doi.org/10.1038/sj.emboj.7601862.

[39] D.U. Mick, M. Vukotic, H. Piechura, H.E. Meyer, B. Warscheid, M. Deckers, et al., Coa3 and Cox14 are essential for negative feedback regulation of COX1 translation in mitochondria, J. Cell Biol. 191 (2010) 141–154, http://dx.doi.org/10.1083/jcb.201007026.

[40] T. Tsukihara, H. Aoyama, E. Yamashita, T. Tomizaki, H. Yamaguchi, K. Shinzawa-Itoh, et al., The whole structure of the 13-subunit oxidized cytochrome c oxidase at 2.8 A, Science 272 (1996) 1136–1144.

[41] L.I. Grossman, M.I. Lomax, Nuclear genes for cytochrome c oxidase, Biochim. Biophys. Acta 1352 (1997) 174–192.

[42] R. Fukuda, H. Zhang, J.-W. Kim, L. Shimoda, C.V. Dang, G.L. Semenza, HIF-1 regulates cytochrome oxidase subunits to optimize efficiency of respiration in hypoxic cells, Cell 129 (2007) 111–122, http://dx.doi.org/10.1016/j.cell.2007.01.047.

[43] J.W. Taanman, R.E. Hall, C. Tang, M.F. Marusich, N.G. Kennaway, R.A. Capaldi, Tissue distribution of cytochrome c oxidase isoforms in mammals. Characterization with monoclonal and polyclonal antibodies, Biochim. Biophys. Acta 1225 (1993) 95–100.

[44] J.W. Taanman, R.A. Capaldi, Subunit VIa of yeast cytochrome c oxidase is not necessary for assembly of the enzyme complex but modulates the enzyme activity. Isolation and characterization of the nuclear-coded gene, J. Biol. Chem. 268 (1993) 18754–18761.

[45] E. Lapuente-Brun, R. Moreno-Loshuertos, R. Acin-Perez, A. Latorre-Pellicer, C. Colás, E. Balsa, et al., Supercomplex assembly determines electron flux in the mitochondrial electron transport chain, Science 340 (2013) 1567–1570, http://dx.doi.org/10.1126/science.1230381.